Experimental study of the influence of electron shell structure on shock adiabats of condensed materials

E. N. Avrorin, B. K. Vodolaga, N. P. Voloshin, G. V. Kovalenko, V. F. Kuropatenko,
V. A. Simonenko, and B. T. Chernovolyuk

Data on the shock compressibilities of aluminum and lead relative to iron are obtained at pressures 35–240 and 80–570 MBar, respectively. These data are the first reliable confirmation that electron shell structure influences the shock adiabats of condensed materials. It is shown that for polyatomic materials, calculations based on the statistical model which include corrections are in better agreement with experimental data than calculations for simple substances.

1. INTRODUCTION

In order to analyze and model processes at high energy densities, one must know the thermophysical properties of condensed materials (equation of state, data on the optical transparency and electron thermal conductivity). The extensive areas of application include the interaction of intense laser, electron, or ion beams with various targets, the theory of strong shock waves, astrophysics, and studies of collisions of fast microparticles with spacecraft.

Until recently, the Thomas-Fermi (TF) statistical model has served as the primary source of simulation data on the thermophysical properties of materials at high pressures $P \gtrsim 100$ Mbar. This model, which incorporates regular quantum-mechanical correction (TFQC) and allows for the nonideal motion of the nuclei, predicts a monotonic dependence of the thermodynamic characteristics on the atomic number Z. However, it neglects the shell structure of the atomic electrons, which causes the thermophysical properties to oscillate as functions of atomic number Z, density ρ, and temperature T and in addition leads to the existence of electron phase transitions.

It has been pointed out in much of the recent theoretical work (see, e.g., the bibliography in Ref. 1) that the electron shell structure has a significant effect on the thermodynamic characteristics even for parameters in the range for which the TF model was formerly thought to be applicable.

Shell effects cause the thermodynamic characteristics (shock adiabats, isochors) to oscillate relative to the monotonic dependence given by the statistical model. If the amplitude of the oscillations is large, the system may become thermodynamically unstable for certain ranges of the thermodynamic parameters; that is, we may have $(\partial^2 P / \partial V^2)_s \leqslant 0$, which is known to be associated with anomalous dynamic behavior in which decompression occurs in the shock wave, while compression occurs monotonically (see, e.g., Ref. 2). Our interest in studying electron shell effects in this paper stems from the fact that a substantial reworking of the algorithms used in existing computer programs would be required in order to treat these anomalies for a wide class of physical phenomena.[3]

2. THEORETICAL MODELS

Under shock conditions the pressure, material density, and other parameters vary over three to six orders of magnitude. Since the properties of the material play an important role throughout this range, it is important to know them precisely.

Although this information can be obtained experimentally in a range of parameters near STP, there is an extremely wide range for which recourse to theoretical models is unavoidable. The oscillation corrections to the TF model are of the same order in $\hbar$ as the regular quantum mechanical corrections, as follows even in the semiclassical approximation (see, e.g., Ref. 4). However, the most reliable models are the ones that proceed from first principles. The development of modern quantum-mechanical models is beset by serious theoretical difficulties which have necessitated a variety of simplifying assumptions. An idea of the difficulties in devising a rigorous theory can be gained by listing the assumptions used in the self-consistent field (SCF) (Ref. 5) and Hartree-Fock-Slater (HFS) (Ref. 6) models, which are currently the best developed: 1) the adiabatic approximation is used to separate the thermodynamic functions into electron and nuclear components; 2) each cell is electrically neutral (correlations among cells are ignored); 3) the cells are spherical (this rules out all uncompressed materials); 4) Slater's method is used to replace the exchange interaction by a "local exchange"; 5) it is assumed that there are energy bands in the vaporized material within which neither long- nor short-range ordering is present; 6) the single-electron approximation is used to treat a many-body problem. The situation is aggravated by the lack of a unified approach to finding the energy bands and describing the nuclear component. Thus, the SCF model uses a quasi-band approximation, while the energy bands in the HFS model are found by using the Bloch periodic boundary conditions for the wave functions; in the model based on the semiclassical equation of state (SCES) (Ref. 7) the width of the band is estimated semiclassically, the electron distribution in the band being taken proportional to the square of the wave quantum number. The nuclear properties are widely described using the ideal gas approximation, which for dense materials breaks down for temperatures $\lesssim 100$ eV, a region of practical interest. In Ref. 8 a Monte-Carlo approach was developed for solving the equations of state for a one-component plasma. When this model was used to treat the thermal-motion of the nuclei, the shock adiabats were found to be shifted to the left in the pressure vs compression plane. The shortcoming of the approximation in Ref. 8 is its assumption of point-like ions. The hard sphere model is used in Ref. 9 to treat the ion interaction for $T \gtrsim 10$ eV; the radius of the spheres is calculated from the density distribution of the bound atomic electrons, i.e., it is temperature-dependent. This method for treating the ion interaction misrepresents the shock adiabats

even more seriously than the previous case.

The simplification used in developing the various models make it difficult to assess their applicability. In addition, it is difficult to judge how a given assumption will affect the thermodynamic functions. Calculations show that in some cases of practical importance, the differences among the thermodynamic quantities calculated using different models are comparable to the entire effect of the shell structure. Figure 1 illustrates the situation for the shock adiabats for the case of aluminum. The shell structure effects are clearly appreciable even where the statistical approach was thought to apply; the departure of the oscillating shock adiabats from one another and from the monotonic (nonoscillating) dependence given by the TFQC model is greatest at pressures ~ 100 Mbar. Although the SCF and HFS models predict similar oscillation phases, the amplitudes on the lower half-wave differ by nearly a factor of two. Curves 1, 3, 4, and 6 in Fig. 1 were calculated using the method in Ref. 8 to treat the nuclear component. Although the SCES model is highly simplistic, it does reflect the basic fact that electrons are combined into shells in real atomic systems, and it yields results whose phase and amplitude agree fairly well with the SCF data. However, a similar situation is found when the ideal gas approximation is used to describe the nuclei (curve 2); the agreement is poorer when the approximation in Ref. 8 is used to treat the nuclei (curve 7).

Figure 1 also shows shock adiabats for aluminum calculated in Ref. 10 using two models developed by American researchers. The ACTEX scheme[11] assumes an ionized equilbrium plasma with an effective electron-ion potential, which is fitted to experimental spectroscopic data. The strong ion-ion interaction is treated in an approximation which yields results similar to those in Ref. 8 in the limit $Z \to \infty$. Where the model applies ($\rho/\rho_0 < 1, T > 2.5$ eV), the ACTEX results lie between the values found by solving the Saha equations with and without the Debye-Hückel correction (see, e.g., Ref. 2). In the region corresponding to ionization of the L-shell on the Al shock adiabat, the electron-electron interaction becomes comparable to the kinetic energy, i.e., the lower halfwave of the oscillation lies outside

the region where the model applies. This accounts for the considerable disagreement between the ACTEX results and those found by other models in this region. The agreement is better at higher pressures (temperatures). The INFERNO model in Ref. 12 is based on the same approximations as the SCF and HFS models. However, the lower portion of the shock adiabat behaves differently because the levels are not split into bands. In the INFERNO model, the effects of the shell structure are in general more pronounced and commence at higher pressures. The splitting of levels into bands permits the gradual escape of electrons into the continuous spectrum, while the high temperatures accompanying the shock compression tend to blur the boundaries of the energy bands. These factors smooth out the effects of ionization on the shock adiabats. Given the limited information available concerning the INFERNO model, it is difficult to explain why the phase of the shock adiabat differs from that found by the other models at pressures above 1000 Mbar.

Most of the available information on thermodynamic functions with shell-structure corrections has come from the SCF and HFS models. Although much effort has gone into the development of numerical algorithms, these models require elaborate calculations even for simple materials. The computational load is much greater for chemically complex materials, for which no SCF or HFS data are currently available.

A simple model, based on using the Bohr-Sommerfeld quantization rules to calculate the bound electron levels in a TF potential, was suggested in Ref. 7 as a quick method for calculating the contribution of shell effects to the thermodynamic functions. Due to its simplicity and computational speed, and because of the fact that the results were calibrated against SCF data for simple materials with various Z, this model merits generalization to calculations of thermodynamic functions for polyatomic materials. Calculations for parameter values of practical interest have shown that the thermodynamic functions for chemically complex materials exhibit more frequent (and in some cases, smaller) oscillations than is found for the corresponding "homogeneous" materials (in which the atomic numbers and nuclear charges have been replaced by their average values). This is illustrat-
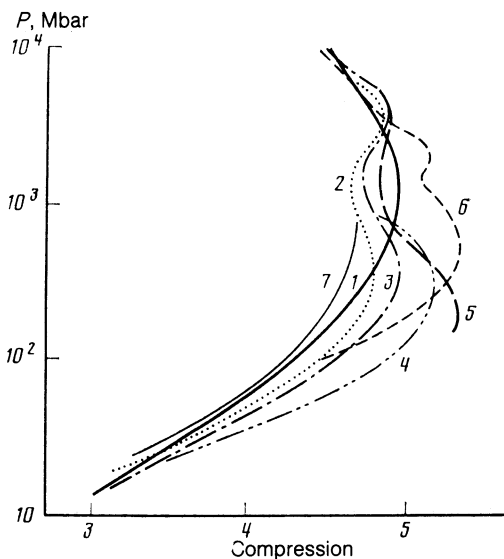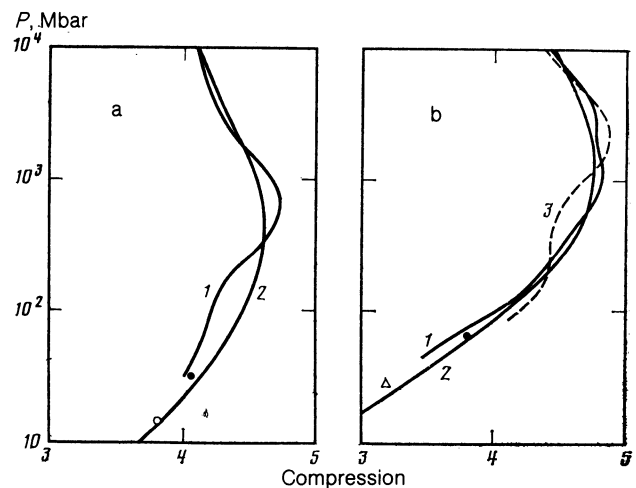

FIG. 1. Shock adiabats for aluminum calculated by various models: 1) TFQC; 2) SCES; 3) SCF; 4) HFS; 5) ACTEX; 6) INFERNO; 7) SCES, with nuclei treated as in Ref. 8.

FIG. 2. Influence of shell effects on shock adiabats for water (a) and quartzite (b): 1) calculated by the SCES model; 2) TFQC; 3) SCES, with A and Z replaced by their average values; $\bigcirc$, $\triangle$ experimental values from Refs. 31, 25, respectively; $\bullet$, our experimental data. For quartzite, 99% SiO_2.

ed in Fig. 2, which presents calculated results for water and quartzite for all parameters of practical interest.

The theoretical models require calibration, and it is necessary to calculate the magnitude of the oscillations in the thermophysical quantities and verify that the conditions for thermodynamic stability are satisfied. It is therefore important to have experimental data for pressures in the ~ 100 Mbar range. At present, the only way to investigate the thermodynamic characteristics of condensed materials at these pressures is to employ shock-wave experiments. The required experimental accuracy is determined by the minimum detectable oscillation amplitude and by the magnitude of the disagreement in the data from the different models.

3. SHOCK-WAVE STUDIES

All of the available experimental data on the thermodynamic properties of dense materials at pressure > 1 Mbar have been obtained in shock-wave experiments, in most cases (see, e.g., Refs. 2, 13) by measuring the shock compressibility of solid and porous specimens during a single or double compression, together with the speed of sound in the shock-compressed material. Isentropic compression has been studied only for a few materials, because the measurements are complicated and too imprecise to be useful for model calibration.

Experiments measuring the compressibility of materials in shock waves are based on formulas derived using mass, momentum, and energy conservation; they relate the kinematic parameters (shock-wave velocity D, mass velocity u in the wake) to the thermodynamic quantities (density, pressure, internal energy). The thermodynamic quantities can be found from simultaneous measurements of D and u without recourse to models. This method has been used to investigate the shock adiabats for only a relatively small number of materials (in the USSR, primarily iron). In the experiments in Ref. 14, a projectile was accelerated to 20 km/s and the pressure in the iron specimens reached 13.5 Mbar. Other techniques are needed to reach the higher pressures needed to compare the models. Two methods for measuring D and u at high pressures were proposed in Refs. 15, 16.

In most experiments, one measures the velocity of a shock wave in two materials which are in physical contact. The procedure for finding the mass velocity in one of the paired materials (the specimen) is based on the $P-u$ diagram method[2] and assumes that the equation of state for the other (reference) material is known. The analysis requires a knowledge of the adiabats for single and double compressions, as well as the decompression isentropes for the reference materials. However, only the shock adiabat for single compression is known experimentally to the required accuracy; the other quantities are found from model calculations, and it is precisely the correctness of these models that must be tested. For this reason it is common practice to replace the isentropes and the shock adiabat for double compression by the mirror image of the shock adiabat for a single compression. If the densities of the reference and specimen change substantially, or if the pressures are high, this simplification causes a large error in the mass velocity inside the specimen.

No single procedure is used in the literature to analyze and estimate the error in calculating the thermodynamic quantities as functions of D, u or P, σ (where $\sigma = \rho/\rho_0$) from

measurements of the wave velocities at the interface between the two materials, expressed in terms of D, D. The equations of state for the reference materials also disagree. It is not unusual for a given specimen to be studied relative to several different reference materials, or for experimental results obtained using model results in the reference to be compared with data from a different model for the specimen. This makes it difficult to systematize and compare experimental data reported by different researchers. Such a comparison would appear to be meaningful only in the D, D plane, because only the wave velocities are directly measurable experimentally. The calculated dependences found by different models should also be expressed in terms of these variables. Although no reference material is needed in this approach, more experimental measurements are required to compare and calibrate the data, because the relative contribution from each material to the discrepancy with the experimental data is unclear $a priori$. Preference should be given to the model whose results, expressed in D, D coordinates, agree best with the experimental data for the largest number of materials.

The choice of D, D variables is also appropriate for another reason. A comparison of various model calculations with the data in Refs. 13 and 14 revealed that starting at pressures $\gtrsim 1$ Mbar, for which the hydrodynamic approximation is valid, and extending up to pressures ~ 1000 Mbar corresponding roughly to the first turning point on the shock adiabats, the relations are nearly linear when expressed in D, D coordinates—the coefficients of the linear terms are ~ 1, while the coefficients of the quadratic terms are 10^{-4}–10^{-5}. In addition to providing an internal check on the experimental data, this also makes it possible to statistically analyze data obtained at different shock wave intensities, assuming enough data points are available. Although statistical averaging reduces the error in the experimental curve as compared with the typical error for each point,[17] it requires measurements for each pair of materials over a wide range of pressures.

The unambigous identification of the reasons for the disagreements between the various theories imposes severe constraints on the accuracy of the experimental data. For example, our calculations show that the effects of electron shell structure on the shock adiabat cannot be detected experimentally unless the wave and mass velocities are measured to within $\lesssim 1\%$. In order to analyze the oscillations on the shock adiabats for materials with large Z (e.g., lead) and calibrate the theoretical models, one must decrease this error further to $\sim 0.5\%$. Moreover, calculations with porosity coefficients ranging from 1 to 50 indicate that the same precision is needed to investigate the compressibility of porous materials.

Measurements from high-explosive experiments yield information at pressure high enough for shell structure effects to be observable. However, the advantage of higher pressures comes at the cost of a considerable modification of the conventional measurement techniques. Although research both in the USSR and abroad[18-25] has demonstrated the feasibility in principle of obtaining data for all pressures of practical interest, in most cases the results have not sufficed for model calibration and analysis of electron shell effects.

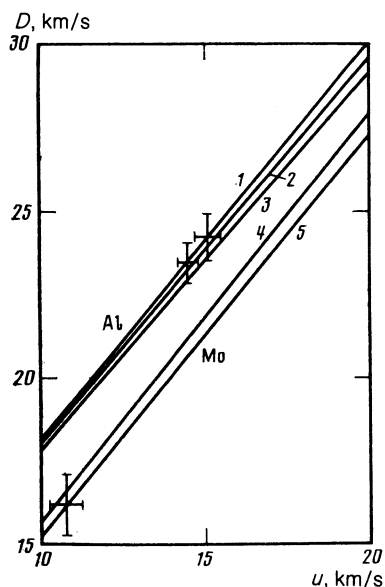Analysis of existing experimental data on the absolute

FIG. 3. Comparison of absolute measurements for aluminum and molybdenum shock adiabats with results found by various models. Experimental results for Al are from Ref. 16, for Mo, from Ref. 15: 1) Ref. 28; 2) Ref. 30; 3) Ref. 29; 4) found by interpolating between the low- and high-pressure data in Refs. 27 and 5, respectively; 5) TFQC. The values for molybdenum are shifted downward by two units along the vertical axis.

FIG. 4. Comparison of experimental data[23-25] with calculated results expressed in D, D coordinates: 1) TFQC; 2) interpolation between the data in Refs. 29 and 5.

compressibility of aluminum[16] and molybdenum[15] indicates that the measurements were carried out at pressures near the threshold for the onset of shell structure effects, so that these effects were small, and the results were not accurate enough to permit choosing one model over another (Fig. 3). Although the absolute methods proposed in Refs. 15, 16 can in principle be made accurate to within $\sim 1\%$ for pressures $P \gtrsim 100$ Mbar, the required measurements are extremely complex and have not yet been carried out.

It is simpler to measure the wave velocities at the interface between two materials. The measurement technique depends on the range of pressures investigated. The methods for exciting shock waves with various intensities and a well-defined profile are familiar to specialists in the field. The arrival of the wave at a control surface can be ascertained by recording the signal accompanying the closing of electrical contacts, deduced from the optical emission from layers of air adjacent to the specimen, or determined from the emission from vaporized material in the decompression wave.[19-22] Each method applies for a certain range of pressures. One must know the damping of the shock wave in order to calculate the wave velocities at the contact surface from their average values; the damping is calculated and is generally monitored experimentally. The method in Ref. 16 is used to calculate corrections for heating (by gamma-photons, e.g.) ahead of the wavefront. The measurement error depends on the recording instruments, the shape of the shock wave channel, the error in measuring the wave damping factor inside the specimens, and the symmetry of the wavefront relative to the measurement surfaces.

The time intervals in Refs. 18, 19 were measured to within 0.7–1.0%, and the wave damping factor was ~ 1–2%. These results can be used for model calibration, but they shed little light on the effects of shell structure because the pressures are too low. Calculations based on various models predict that the electron shells should alter the shock
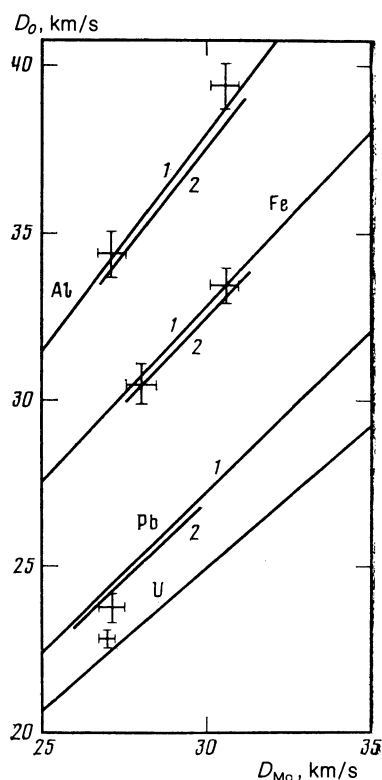
adiabats only slightly, and the resulting D, D dependences are straight-line segments which are separated along the ordinate axis but have slopes that depend only very slightly on the model.

Roughly the same pressures were achieved in American experiments,[23-25] where pairs containing a molybdenum specimen were studied (in most cases, the wave was incident first on the Mo plate). The error in measuring the wave velocities was 1.4–2.6%, depending on the specimen, and the correction for damping was less than 2%. In addition to this correction, they also allowed for the distortion of the shock wavefront at the location of the apparatus, an assembly (or cage) of plane-parallel plates. The measurements were analyzed there in terms of P, u diagrams. Several further conclusions can be reached by reexpressing these data in terms of D, D coordinates (Fig. 4). First of all, the relationship of the calculated results to the experimental data in Refs. 23, 24 is striking. The measured velocities in lead and uranium lie on opposite sides of the curves found by the TFQC model,[26] so that the difference between them is just one-half the calculated value. Although this could be due to shell structure effects, the amplitude and position of the oscillations on the shock adiabats for lead and uranium disagree with our experimental data[27] and with the predictions of all other models. The slope of the lines joining the experimental points for Mo–Fe and Mo–Al differs appreciably from the calculated value. An unambiguous explanation is not possible due to the limited amount of experimental information.

Several new ideas for reaching pressures ~ 100 Mbar were tested experimentally in Ref. 20. However, the measurement error was larger than expected and was due primarily to errors in correcting for wave damping inside the

experimental apparatus. The results are therefore not suitable for model calibration. Still higher experimental pressures were reached in Ref. 21 by replacing the flat system in Ref. 20 by a spherical one. However, the shock wave damping in the specimens was thereby increased, and uncertainties in correcting for this again gave the dominant contribution to the measurement error.

Novel methods of measurement for analyzing the effects of electron shell structure were used in Ref. 22, where the shock wave transit times, measured experimentally for different specimen materials, were compared with values calculated by the technique in Ref. 28. The pressure at the wavefront dropped by a factor of 3–4 during propagation between the specimens, i.e., the decompression isentropes as well as the shock adiabat must be known in order to model the conditions of wave propagation. Since at these pressures these are the very characteristics most in need of calibration, it remains unclear if such measurements can be interpreted unambiguously. The measurement error cited in Ref. 27, for example, is too large for the oscillations to be detected experimentally.

4. MEASUREMENT METHOD AND RESULTS

We developed techniques for achieving the required precision based on an analysis of the measurements in Refs. 20, 21, and the new measurements were performed in 1983 (Ref. 27). Shock waves with a well-defined wavefront shape were excited in a test cage containing a 2.5-cm-thick reference plate on which the specimens, of thickness ~ 1 cm, were placed. The measurements were carried out for several pressures at the wavefront without changing the experimental configuration. The measurement baselines were chosen so that the wave velocities did not oscillate inside the plates, in agreement with the calculations. The design of the cage ensured that the plates were parallel. The plates in the cage were fabricated under precisely controlled conditions (for example, they were microscopically smooth to within 2.5 μm), and their density and thickness were measured to high precision.

The instants when the wavefront reached the measurement surfaces were determined from the optical emission from the adjacent layers of air. This emission was recorded along optical channels which contained photocathode detectors and had inner walls of polished metal. The precision of the measurements was improved by positioning the three measurement surfaces, chosen to correspond to the desired

pressure (two for the reference, one for the specimen), in the viewing field of a single photocathode. Two layers of identical material were inserted in order to measure the wave damping experimentally. Opaque barriers in the optical channel prevented mutual illumination of the surfaces. Two detectors were placed in each optical channel, and each detector recorded the signal completely. The complex, three-step structure of the signal required the use of an oscilloscope. The time intervals were measured more accurately by using a recording scheme in which the emission signals were recorded by using short sweeps and precisely known delays. State-of-the-art computer techniques and data-processing routines were used to read and analyze the signals from the oscilloscope traces. Based on the wave amplitude anticipated in the experiment, we varied the length and coating of the channel so as to ensure that the photodetectors operated on the linear portion of their characteristic.

The measurements were carried out for the following pairs of materials: iron–aluminum, iron–lead, lead–iron, iron–water, iron–quartzite. The wave was incident on the first member of each pair. The choice of material was motivated by the following considerations. Aluminum is of interest because of the relative ease with which pressures corresponding to the lower halfwave of the oscillations on the shock adiabat can be achieved, and because the oscillation amplitude is large. Various theoretical models indicate that this amplitude should decrease with increasing atomic number. Based on experience in prior investigations, we chose lead as the high-Z material.

The shell effects do not depend monotonically on Z. Therefore, for compounds containing atoms with different Z these effects may be enhanced for certain values of p, T and decreased for others. The calculations for complex materials are much more laborious than for simple ones. Recalling our discussion of theoretical models in Sec. 2, we see that the problem of calibrating a single model capable of describing the role of electron shell effects in complex materials becomes even more acute. This was our motivation for investigating the shock compressibility of water and quartzite.

The magnitudes of the wave velocities were determined directly on the measurement surfaces, and the corresponding values on the contact interfaces were determined numerically. The damping corrections ranged from 2 to 8% and depended on the material, being largest for lead. The algorithm for solving the gasdynamic equations employed a difference scheme with a variable stepsize, smaller at the

TABLE I. Wave velocities (km/s) at the contact interface.

	Wave velocities				
Iron–aluminum	88.20±0.7	71.25±0.6	66.74±0.6	62.65±0.6	54.90±0.6
	42.63±0.7	41.79±0.6	36.77±0.5	–	–
	107.1±0.9	85.98±0.8	80.11±0.8	75.03±0.7	65.22±0.6
	50.58±0.7	49.59±0.7	43.57±0.6	–	–
Iron–lead	89.6±1	88.20±0.7	71.25±0.6	66.74±0.6	62.65±0.6
	54.90±0.6	43.6±1	42.63±0.7	41.79±0.6	36.77±0.5
	78.4±1	76.70±0.7	61.33±0.7	56.98±0.6	53.43±0.6
	46.60±0.5	36.3±1	35.44±0.6	35.00±0.6	30.42±0.5
Lead–iron	63.11±0.6	49.09±0.6	–	–	–
	72.58±0.7	57.07±0.6	–	–	–
Iron–water	45.54±0.7	–	–	–	–
	64.10±0.7	–	–	–	–
Iron–quartzite	45.90±0.7	–	–	–	–
	55.98±0.7	–	–	–	–

strong shock fronts, and conductive and adiabatic flow models were both treated. The accuracy of the calculated corrections was checked in the experiments. Table I lists the wave velocities at the contact interface between each pair. The total error (in percent) corresponding to a 0.95 confidence probability is also shown. Most of the error in the wave velocities was caused by errors in time measurement due to the finite width of the oscilloscope beam.

5. DISCUSSION OF THE MEASUREMENTS

The calculated dependences found by the various models for our pairs of materials are plotted in D, D coordinates in Fig. 5, which also shows the measured wave velocities (including errors). Under our conditions, the maximum difference between the calculated dependences is 1.4–3.4 km/s for aluminum and 1.2–2.3 km/s for lead, which is less than the measurement error. Statistical analysis of the experimental data enabled us to decrease the error in measuring the oscillation amplitude by a factor of three as compared with the error for a single point. These results (Fig. 6) show that the shock adiabats for aluminum and lead are clearly affected by the electron shell structure. Both the oscillation amplitude and its falloff with increasing atomic number correlate well with the predictions of the SCF model, in which the widths of the energy bands responsible for the thermodynamic behavior are calculated in the quasiband approximation; this procedure is quite similar to the one employed in the statistical model based on the smeared electron shell approximation. If anything, the experimentally measured half-wave of the oscillations was more compressed along the pressure axis than predicted by the calculations.

It is clear that the more closely the model and experimental data agree when the results are expressed in terms of D, D coordinates, the better the corresponding shock adiabats will agree when expressed in terms of compression vs pressure. The characteristic magnitude of the discrepancies is shown in Fig. 7, which shows the results found by analyzing the experimental data for iron–aluminum and iron–lead; for comparison, data obtained from the TFQC models and by interpolation between the SCF data and the data from the phenomenological method in Ref. 29 are also shown. Iron
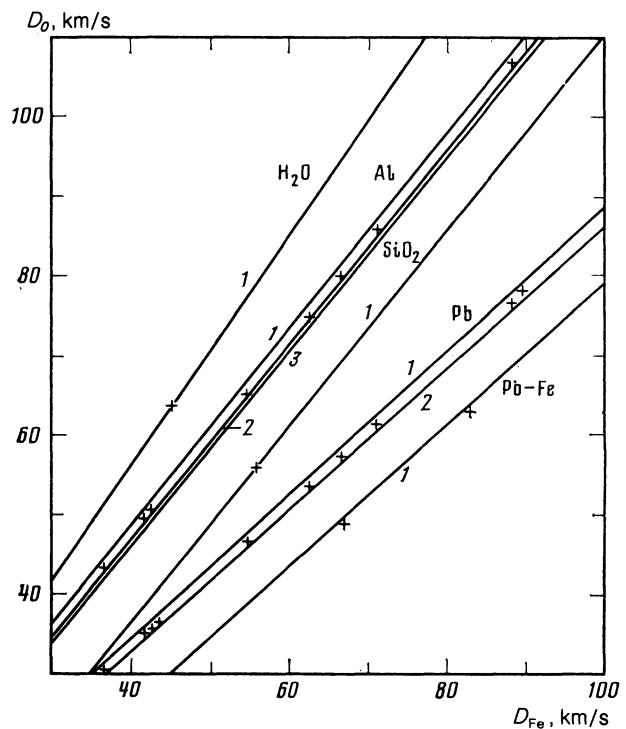
FIG. 5. Comparison of our experimental data with results found using other models, expressed in D, D coordinates: 1) TFQC; 2) interpolation between the data in Refs. 29 and 5; 3) Ref. 29. The results for ion–quartzite and lead-iron are shifted one unit to the right along the horizontal axis.

was taken as the reference material in this analysis.

Since studies of the dynamic compressibility of complex polyatomic materials have only just begun, it would be premature to make any final assessment. Calculations using the model in Ref. 7 showed (Fig. 2) that for water, the effects of electron shell structure become appreciable at pressures of ~100 Mbar; for quartzite, the shell effects at these pressures are even more pronounced (the oscillations of the oxygen and silicon atoms nearly cancel out). These experimental results are consistent with the calculated data.

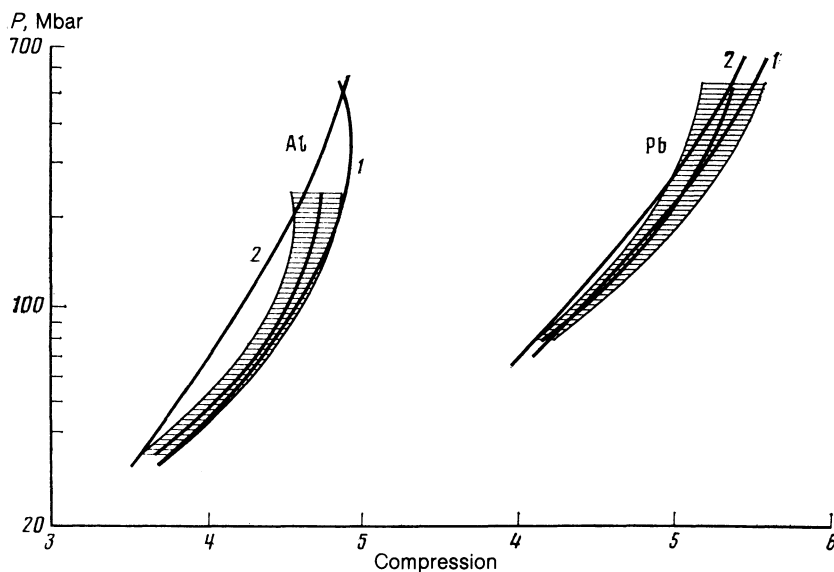Our experiments differed in several respects from ear-

FIG. 6. Results from a least-squares analysis of our data. The nominal position of the shock adiabats is in the center of the hatched regions (error bars): 1) shock adiabats calculated by interpolating between the values in Refs. 29 and 5; 2) found by the TFQC model.
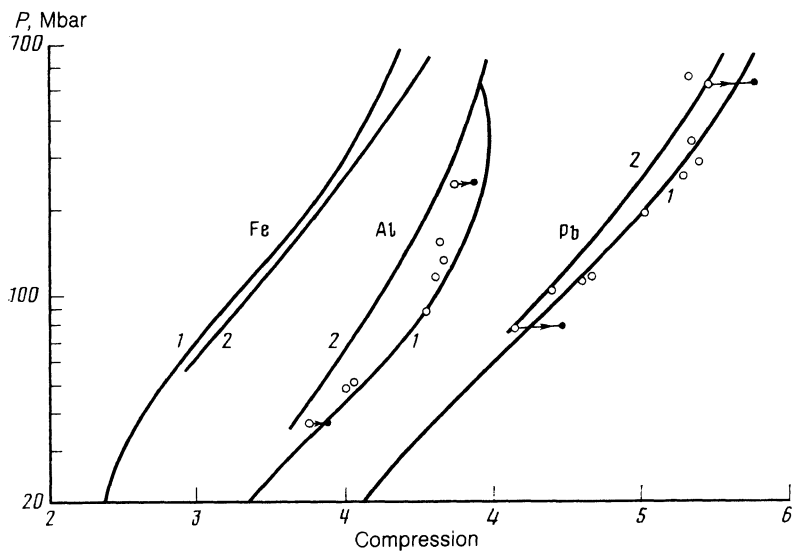
P, Mbar

FIG. 7. Results found from a P, u diagram analysis of experimental data for ion–aluminum and iron–lead. $\bigcirc$ and $\bullet$ gives values for the reference material (iron) found by interpolating the results in Refs. 29, 5, and by using the TFQC models for iron, respectively: 1) shock adiabats calculated using data in Refs. 29, 5; 2) TFQC model.

lier ones. In particular, due to the sharpness of the shock wavefront in the experimental cages, the damping corrections were somewhat larger (see above for specific values), the plates were heated to a higher temperature ($\lesssim 0.1$ kJ/g), and a different method was needed to output the data. A comparison of the data with the earlier results is therefore warranted. For iron–lead, the wave velocity values in Refs. 18, 19 are the closest to ours. Figure 8 compares those values (+) with the results found from a least-squares interpolation of the data in Table I at low pressures: $D_{\mathrm{Pb}} = -1.3452 + 0.8495 D_{\mathrm{Fe}} + 4.01 \cdot 10^{-4} D_{\mathrm{Fe}}^{2}$. The agreement with the experimental wave velocities for lead is seen to be better than a few tenths of one percent.

For iron–aluminum, extrapolation gives a poorer fit, because the maximum pressures (and hence velocities) were recorded for quartzite–aluminum ($P = 20.48$ MBar) in Ref. 19 but for molybdenum–aluminum ($P = 22.3$ Mbar) in Refs. 24, 25. The following wave velocities (km/s) were recorded by the electrical contact method at an iron–aluminum interface:

| Iron | 11.69 | 12.90 | 15.02 | 16.17 | 17.08 | 22.69 |
| Aluminum | 13.87 | 15.59 | 17.81 | 19.17 | 19.75 | 26.45 |

These data are compared in Fig. 8 with the results ob-
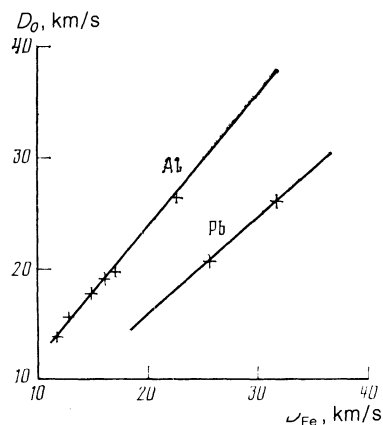

D_0, km/s

FIG. 8. Comparison of our results with values recorded using electrical contacts, expressed in D, D coordinates. The lines show the dependence $D_0(D_{\mathrm{Fe}})$ found by a least-squares extrapolation based on the data in Table I. Experimental values (+) for iron-lead (Refs. 18, 19) and iron-aluminum (our results) are shown.

tained by extrapolating to lower wave velocities the dependence given by the data in Table I ($D_{\mathrm{Al}} = 0.6140 + 1.1377 D_{\mathrm{Fe}} + 8 \cdot 10^{-4} D_{\mathrm{Fe}}^{2}$). The experimental results are seen to agree closely at low pressures.

At higher pressures, our results for iron–aluminum are consistent with the experimental point found in Ref. 21: $D_{\mathrm{Fe}} = 120 \pm 2$ km/s, $D_{\mathrm{Al}} = 147 \pm 2$ km/s, and $P_{\mathrm{Al}} = 460$ Mbar.

In our measurements the time intervals were measured between signals of identical nature, so that there is little need to include corrections for the finite time the air layer requires to stop radiating—in addition to being very small, these corrections are also virtually identical for each measurement surface. Indeed, if we write l for the mean free path (averaged over the spectrum) in air at normal density and take $\sim 3l$ as the distance the wave must travel in air before emission stops, we get a correction $\Delta t = 3l/\sigma(D - u) = 3l/D$ to the time, where D is the velocity with which the wave enters the air. Since D was at least ≈ 80 km/s in our measurements, the temperature behind the wavefront was $\sim 1.5 \cdot 10^{5}$ K, and l was 10^{-4} cm (Ref. 2), we obtain $\Delta t \approx 0.04$ ns.

Our calculations reveal that at low densities, the position and amplitude of the oscillations found using the SCF model agree with the data obtained by solving a system of Saha equations containing experimentally determined spectroscopic parameters (i.e., using information about the electron shell structure). Agreement with experiment is also observed at solid-state densities. We expect that the model is also valid for the intermediate densities as yet inaccessible to experiment. The predictions of the SCF model concerning the oscillation amplitudes of the thermodynamic functions can be used to investigate whether the condition $(\partial^{2}P/\partial V^{2})_{s} > 0$ is satisfied for parameter values of practical interest. Such an analysis was carried out for aluminum by N. M. Baryshev and G. V. Sin'ko, whose calculations demonstrate that the condition for thermodynamic stability holds throughout the region of practical interest. This lends weight to the correctness of the numerical results found using existing simulation algorithms.

[1]V. A. Simonenko, Topics in Atomic Sciences and Technology, Ser. Teor. Prikl. Fiz., Vol. 1 (1984), p. 3.

[2]Ya. B. Zel'dovich and Yu. P. Raĭzer, *Fizika Udarnykh Voln i Vysoko-temperaturnykh Gidrodinamicheskikh Yavleniĭ (Physics of Shock Waves and High Temperature Hydrodynamic Phenomena),* Academic Press, New York (1966, 1967).

[3]B. L. Rozhdestvenskiĭ and N. N. Yanenko, *Sistemy Kvasilineĭnykh Uravneniĭ i ikh Prilozheniya v Gazovoĭ Dinamike (Systems of Quasilinear Equations and Applications to Gas Dynamics),* Nauka, Moscow (1968).

[4]D. A. Kirzhnits, Yu. E. Lozovik, and G. V. Shpatakovskaya, Usp. Fiz. Nauk **117**, 3 (1975) [Sov. Phys. Usp. **18**, 649 (1975)].

[5]G. V. Sin'ko, Chisl. Met. Mekh. Sploshn. Sred **10**, 124 (1979).

[6]A. F. Nikiforov, V. G. Novikov, and V. G. Uvarov, Topics in Atomic Science and Technology, Ser. Metody i Programmy Chisl. Resheniya Zadach Mat. Fiz., Vol. 4(6) (1979), pp. 16, 27.

[7]A. V. Andriyash and V. A. Simonenko, Topics in Atomic Science and Technology, Ser. Teor. Prikl. Fiz., Vol. 2(2) (1984), p. 52.

[8]V. P. Kopyshev, Chisl. Met. Mekh. Sploshn. Sred **8**, 54 (1977).

[9]V. G. Novikov, Inst. Prikl. Mat. AN SSSR Preprint No. 33 (1986).

[10]D. A. Young, J. K. Wolford, F. J. Rogers, and K. S. Holian, Phys. Lett. A **108**, 157 (1985).

[11]F. J. Rogers, Phys. Rev. A **24**, 1531 (1981).

[12]D. A. Liberman, J. Quant. Spectr. Rad. Transfer **27**, 335 (1982).

[13]L. V. Al'tshuler, Usp. Fiz. Nauk **85**, 197 (1965).

[14]L. V. Al'tshuler, A. A. Bakanova, I. P. Dudoladov, *et al.*, Prikl. Mekh. Tekh. Fiz., No. 2, 3 (1981).

[15]C. E. Ragan III, M. G. Silbert, and B. C. Diven, J. Appl. Phys. **48**, 2860.

[16]V. A. Simonenko, N. P. Voloshin, A. S. Vladimirov, *et al.*, Zh. Eksp. Teor. Fiz. **88**, 1452 (1985) [Sov. Phys. JETP **61**, 869 (1985)].

[17]N. N. Kalitkin and L. V. Kuz'mina, Inst. Prikl. Mekh. AN SSSR Pre-print No. 116 (1985).

[18]L. V. Al'tshuler, B. N. Moiseev, L. V. Popov, *et al.*, Zh. Eksp. Teor. Fiz. **54**, 785 (1968) [Sov. Phys. JETP **27**, 720 (1968)].

[19]R. F. Trunin, M. A. Podurets, G. V. Simakov, *et al.*, Zh. Eksp. Teor. Fiz. **62**, 1043 (1972) [Sov. Phys. JETP **35**, 550 (1972)].

[20]E. N. Avrorin, B. K. Vodolaga, L. P. Volkov, *et al.*, Pis'ma Zh. Eksp. Teor. Fiz. **31**, 727 (1980) [JETP Lett. **31**, 685 (1980)].

[21]A. S. Vladimirov, N. P. Voloshin, V. N. Nogin, *et al.*, Pis'ma Zh. Eksp. Teor. Fiz. **39**, 69 (1984) [JETP Lett. **39**, 82 (1984)].

[22]I. Sh. Model', A. T. Narozhnyĭ, A. I. Kharchenko, *et al.*, Pis'ma Zh. Eksp. Teor. Fiz. **41**, 270 (1985) [JETP Lett. **41**, 332 (1985)].

[23]C. E. Ragan III, Phys. Rev. A **21**, 458 (1980).

[24]C. E. Ragan III, Phys. Rev. A **25**, 3360 (1982).

[25]C. E. Ragan III, Phys. Rev. A **29**, 1391 (1984).

[26]N. N. Kalitkin and L. V. Kuz'mina, Inst. Prikl. Mekh. AN SSSR Pre-print No. 14 (1976).

[27]E. N. Avrorin, B. K. Vodolaga, N. P. Voloshin, *et al.*, Pis'ma Zh. Eksp. Teor. Fiz. **43**, 241 (1986) [JETP Lett. **43**, 308 (1986)].

[28]G. M. Eliseev and G. E. Klinishov, Inst. Prikl. Mekh. AN SSSR Pre-print No. 173 (1982).

[29]A. T. Sapozhnikov and A. V. Pershina, Topics in Atomic Science and Technology, Ser. Metod. i Programmy Chisl. Resheniya Zadach Mat. Fiz., Vol. 4(6) (1979), p. 47.

[30]V. F. Kuropatenko and I. S. Minaeva, Chisl. Met. Mekh. Sploshn. Sred **13**, 69 (1982).

[31]M. A. Podurets, G. V. Simakov, R. F. Trunin, *et al.*, Zh. Eksp. Teor. Fiz. **62**, 710 (1972) [Sov. Phys. JETP **35**, 375 (1972)].

Translated by A. Mason